# CHAPTER 4

# STUDY THE EFFECTS OF TEMPERATURE AND STRAIN RATES ON TRANSIENT THERMOMECHANICAL RESPONSES ON MULTI-LAYER SKIN TISSUE

## 4.1 Introduction[1]

In various medical treatments, such as laser hyperthermia, coagulation, and surgery, there is a transient heat flux on the skin's surface. A slight change in temperature and stress influences the body's immune system to some extent, alters the rate at which hormones are produced, and deactivate proteins in biological tissue. Moreover, heat transport in active biological tissue is an intricate process which includes thermal conduction in vascular system and tissue, convection among tissue and blood due to blood flow/perfusion via capillaries inside the tissue, metabolic heat production, sweating, energy dissipation through hair, and so forth. During thermal therapy, one of the major concerns is to identify the physical and mechanical property of tissue and apply the right amount of heat for appropriate duration of time to the patient's specific region of the body under study. If the temperature level rises excessively or kept hold for prolonged period of time then severe negative consequences can be observed. Therefore, in order to have better treatment accuracy and for safety purpose, it is very crucial to have the right prediction of temperature and stress field of the entire treatment zone. Several research work have been attempted to model this aspect related to skin tissue.

[1]The content of this chapter is published in *European Journal of Mechanics A/Solid*, 100 (2023): 105028

It is worth recalling that Pennes (1948) had firstly modeled the heat transport mechanism in skin tissue. That investigation used a diffusion type model of the bioheat transport equation based on classical Fourier's law. Its simplicity and applicability to the majority of medical applications, including surgery and chemotherapy, blood perfusion estimates, hyperthermia therapy, and whole-body thermal simulation, make this model intriguing and noteworthy. However, in recent studies, it has been reported that this model fails to explain certain specific situations when large heat flux or quick response time is involved, or when the heat-conduction behaviour exhibits non-Fourier characteristics like the thermal wave phenomena. Richardson et al. (1950) and Roemer et al. (1985) were the first to notice temperature oscillation in living tissue. After conducting several experiments, Liu et al. (1996; 1997) authenticated that temperature oscillations could be properly fitted with temperature wave analysis. Mitra et al. (1995) conducted four distinct tests with processed meat for various boundary conditions and detected the wave-like behaviour of heat transport. Davydov et al. (2001) observed experimentally that heat transport in muscle tissue under local intense heating exhibits significant anisotropy, that cannot be described by the Fourier's law based diffusion model. This drawback motivates the researchers to modify Pennes theory. Modern medical technological advancement demonstrates that the body under various thermal shock loads like laser, ultrasound, burns and so forth shows heat induced deformation on skin tissue. It has been further reported that the body tissues exhibit distinct results of fields (temperature, displacement and stress) under generalized thermoelastic models in comparison to the pure heat conduction model or the classical thermodynamical theories of continua, due to the consideration of interrelationship between thermal and mechanical fields. There are several bioheat transfer models based on generalized thermoelasticity theory as available in the literature: Xu et al. (2008a; 2008b; 2008c) constructed a mathematical model for the skin tissue and studied the coupled thermal and mechanical behaviour and concluded that thermal pain depends on thermal stress

induced by external heat source. Further, Li et al. (2018a; 2018b; 2019) investigated the transient thermomechanical response of skin tissue when the skin properties vary with temperature, through various generalized thermoelastic theory involving the G-N model, fractional order model and DPL model. Zhang et al. (2021) examined the responses of skin tissue in the framework of three phase-lag model and observed that rate of thermal conductivity affects the speed of thermal wave propagation. In the published literature, some interesting results on bioheat transfer models are reported (see Wang et al. (2021), Kumar et al. (2016; 2016), Xu et al. (2008a; 2008b; 2008c), Das et al. (2013), Zhou et al. (2009), Li et al. (2019), Ng et al. (2009; 2010), Vlase et al. (2017) and Alzahrani et al. (2020)).

In this Chapter, we explore the impact of both strain rate and temperature rate factors on transient thermomechanical responses on triple-layered skin tissue through MGL model. As mentioned in previous chapters, this thermoelastic model introduces two thermal relaxation parameters with the strain-rate and temperature-rate factors and modifies the entropy relation and stress-strain temperature relation by keeping the Fourier law of heat conduction unchanged. In order to study the effects of strain and temperature-rates in the thermoelastic behaviour of skin tissue, the present investigation aims to compare the results of MGL model with the results of the DPL model that also involves two phase-lag parameters in the modification of Fourier's law of heat conduction. Here the basic governing equations and constitutive relations of the MGL (Yu et al. (2018)) and DPL models (Tzou (1995b)) are considered in a unified manner by using some constant parameters to make it easier to move between two different models and compare the effects of phase-lags with thermal relaxation terms. We obtain the fundamental solution by applying Laplace transform approach. Laplace inversion based on the Stehfest algorithm (Stehfest (1970)) is carried out to find the numerical solutions for temperature and stress fields and demonstrate the results graphically by using MatLab software. The results are discussed in details. Our comparison indi-

cates how the strain-rate and temperature-rate terms in constitutive relations play a significant role on the behaviour of field variables.

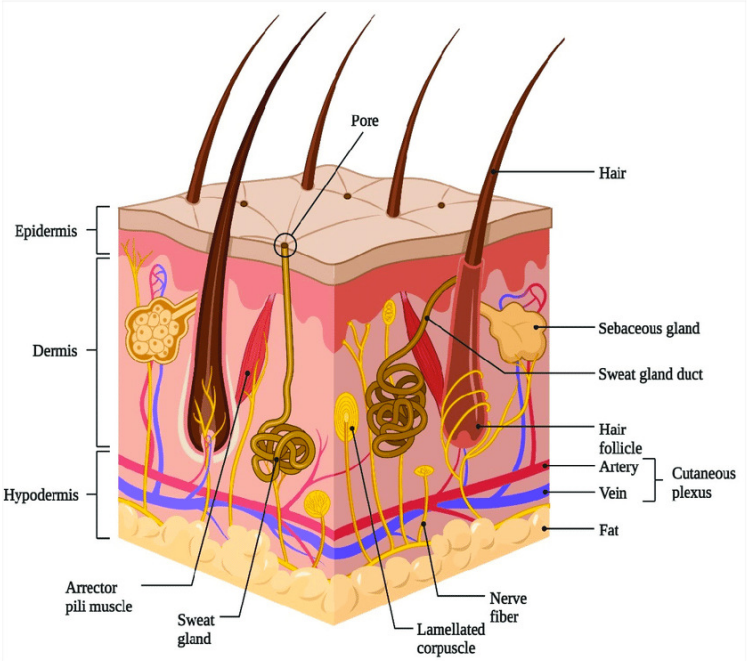


Figure 4.1.1: Layer of skin structure

## 4.2 Mathematical Formulation of the Problem

The present work deals with the investigation of the effects of thermal load on the surface of human skin tissue which consists of three layers namely, epidermis, dermis, and hypodermis layers as shown in figure (4.1.1). It is assumed that the medium is linear, homogeneous and has isotropic thermomechanical characteristics. Blood perfusion occurs only within the dermis and hypodermis layers. As a result, in epidermal layer, blood perfusion has no contribution to thermal effect. The mathematical framework for thermoelastic models of MGL and DPL in conjunction with Penne's bioheat conduction equation is presented in a unified way and represented by the following governing equations (Li et al. (2019); Wang et al. (2021); Yu et al. (2018)) :

The general bio-heat transfer equation:

$$\rho T_0 \frac{\partial S}{\partial t} = -q_{i,i} + \rho_b w_b c_b \left(T_b - T\right) + Q_m. \tag{4.2.1}$$

Generalized heat conduction law:

$$\left(1 + z_3 \tau_q \frac{\partial}{\partial t}\right) q = -\kappa \left(1 + z_4 \tau_T \frac{\partial}{\partial t}\right) \nabla T. \tag{4.2.2}$$

The entropy constitutive equation:

$$\rho T_0 S = \left(1 + z_2 \tau_0 \frac{\partial}{\partial t}\right) \left[\rho c_E T + \gamma T_0 e_{ij}\right]. \tag{4.2.3}$$

The equation of motion:

$$\sigma_{ij,j} = \rho \frac{\partial^2 u_i}{\partial t^2}. \tag{4.2.4}$$

Stress-strain-temperature constitutive relation:

$$\sigma_{ij} = \left(1 + z_1 \tau_1 \frac{\partial}{\partial t}\right) \left(2\mu e_{ij} + \lambda e_{kk} \delta_{ij} - \gamma \theta\right). \tag{4.2.5}$$

where the partial derivatives in relation to cartesian coordinates is symbolized by the comma in the lower right corner (,). $\sigma_{ij}, e_{ij}, u_i$ and $q_i$ represent the component of stress, strain, displacement and heat flux vector, respectively. $\theta$ represents the temperature above ambient reference temperature $T_0$. Lame's constants are $\mu$ and $\lambda$. The terms $c_E$ and $\rho$ stand for specific heat of tissue per unit mass and density. $\gamma$ denotes thermal modulus, and its connection to thermal expansion coefficient $\alpha_t$ is given by $\gamma = (3\lambda + 2\mu)\,\alpha_t \delta_{ij}$. The term $Q_m$ denotes metabolic heat generation in tissue cell. $n$ represents the specific entropy. $\tau_T, \tau_q, \tau_0$ and $\tau_1$ represent the relaxation time parameter/phase-lag parameter. The metabolic heat production of tissue is not taken into account in this study. As a result, $\rho_b w_b c_b \left(T_b - T\right)$ is the only volumetric heat source

left behind in the above-mentioned Eq.(4.2.1). The blood perfusion rate ($w_b$) in this instance indicates how effectively thermal energy is exchanged between the blood and the damaged tissue. Blood's mass density and specific heat capacity are both expressed as $\rho_b$ and $c_b$ respectively.

Based on different sets of values of $z_1, z_2, z_3$ and $z_4$, one can switch from one model of generalized thermoelasticity to another very easily as follows:

**Case I** : MGL model: $z_1 = z_2 = 1; z_3 = z_4 = 0$.

**Case II** : DPL: $z_1 = z_2 = 0; z_3 = z_4 = 1$.

On combining Eqs. (4.2.1-4.2.3), we have

$$k\left\{1 + z_4\tau_T\frac{\partial}{\partial t}\right\}T_{,ii} = \left\{1 + z_3\tau_q\frac{\partial}{\partial t}\right\}\left[\left\{1 + z_2\tau_0\frac{\partial}{\partial t}\right\}\left\{\rho c_E\frac{\partial T}{\partial t} + \gamma T_0\frac{\partial e_{ij}}{\partial t}\delta_{ij}\right\}\right.$$
$$\left. -\rho_b w_b c_b\left(T_b - T\right)\right] \tag{4.2.6}$$

Further, on combining Eqs. (4.2.4) and (4.2.5), we have

$$\rho\frac{\partial^2 u_i}{\partial t^2} = \left\{1 + z_1\tau_1\frac{\partial}{\partial t}\right\}\left(2\mu e_{ij} + \lambda e_{kk}\delta_{ij} - \gamma\theta\right)_{,j}. \tag{4.2.7}$$

Considering the difficulty in computing the 3-D solution for aforementioned set of equationss, the one-dimensional approach is sufficient to explain the characteristics of thermoelastic responses in skin tissue. In order to address the physics of the actual problem, Xu et al. (2008b) assumed the triple-layered skin tissue which consists of the epidermis, dermis and hypodermis layer of length $L_1, L_2$ and $L_3$ respectively. We assume that heat primarily flows along the normal direction to the skin surface, therefore the physical field variables can be taken as functions of coordinate $x$ and time $t$. As a result, we consider the following components of displacement vector:

$$u_y = u_z = 0, u_x^i = u^i(x,t) \tag{4.2.8}$$

where $i = 1, 2, 3$ correspond to the skin tissue layers.

The dilatation $e$ is given by

$$e = e_{xx} = \frac{\partial u}{\partial x}, \tag{4.2.9}$$

and other strain components are zero.

Using Eqs. (4.2.5), (4.2.8) and (4.2.9), the stress components can be expressed as

$$\sigma_{xx}^{i} = \left(1 + z_1 \tau_1 \frac{\partial}{\partial t}\right) \left(\left(\lambda + 2\mu\right) \frac{\partial u^i}{\partial x} - \gamma^i \theta^i\right), \tag{4.2.10}$$

$$\sigma_{yy}^{i} = \sigma_{zz}^{i} = \left(1 + z_1 \tau_1 \frac{\partial}{\partial t}\right) \left[\lambda \frac{\partial u^i}{\partial x} - \gamma^i \theta^i\right] \tag{4.2.11}$$

where $\gamma = \left(3\lambda + 2\mu\right) \alpha_t$.

In view of Eqs. (4.2.8) and (4.2.9), the Eqs. (4.2.6) and (4.2.7) reduce to

$$k^i \left(1 + z_4 \tau_T \frac{\partial}{\partial t}\right) \frac{\partial^2 T^i}{\partial x^2} = \left(1 + z_3 \tau_q \frac{\partial}{\partial t}\right) \left[\left(1 + z_2 \tau_0 \frac{\partial}{\partial t}\right) \left(\rho^i c_E^i \frac{\partial T^i}{\partial t} + \gamma^i T_0 \frac{\partial^2 u^i}{\partial t \partial x}\right) - \left(\rho_b w_b c_b \left(T_b - T^i\right)\right)\right] \tag{4.2.12}$$

$$\rho^i \frac{\partial^2 u^i}{\partial t^2} = \left(1 + z_1 \tau_1 \frac{\partial}{\partial t}\right) \left(\left(\lambda^i + 2\mu^i\right) \frac{\partial^2 u^i}{\partial x^2} - \gamma^i \frac{\partial \theta^i}{\partial x}\right). \tag{4.2.13}$$

Throughout this investigation, we will assume that the initial conditions are homogenous implying

$$T^i\left(x, 0\right) = T_0, \frac{\partial T^i}{\partial t}\left(x, 0\right) = 0, u^i\left(x, 0\right) = 0, \frac{\partial u^i}{\partial t}\left(x, 0\right) = 0. \tag{4.2.14}$$

Boundary conditions are assumed as

$$T^I\left(0, t\right) = T_1 H\left(t\right), T^{III}\left(L, t\right) = T_c, \sigma_{xx}^{I}\left(0, t\right) = \sigma_{xx}^{III}\left(L, t\right) = 0 \tag{4.2.15}$$

here $T_1$ denotes the surface temperature load and $T_c$ denotes the core temperature of arterial blood.

Now, in order to have simplicity in formulation, we introduce non-dimensional variables and similarity standard as follows:

$$(x^*, h^*, L^*) = c_0 n\,(x, h, L)\,, u^* = c_0 n \frac{(\lambda + 2\mu)}{\gamma T_0} u, (t^*, \tau_0^*, \tau_1^*) = c_0^2 \eta\,(t, \tau_0, \tau_1)\,,$$

$$(\sigma_{xx}^*, \sigma_{yy}^*) = \frac{(\sigma_{xx}, \sigma_{yy})}{\gamma T_0}, T^* = \frac{T - T_0}{T_0}, T_b^* = \frac{T_b - T_0}{T_0}, \theta^* = \frac{\theta}{T_0}, Q_m^* = \frac{Q_m}{\rho c T_0 c_0^2 \eta}, q^* = \frac{q}{c_0 \eta k T_0}.$$

The Eqs. (4.2.10-4.2.13) can therefore be converted to the dimensionless forms as shown below ( where we omit the '$*$' for simplicity):

$$\sigma_{xx}^i = \left(1 + z_1 \tau_1 \frac{\partial}{\partial t}\right) \frac{\lambda^i + 2\mu^i}{\lambda + 2\mu} \frac{\partial u^i}{\partial x} - \left(1 + z_1 \tau_1 \frac{\partial}{\partial t}\right) \frac{\gamma^i}{\gamma} \theta^i \tag{4.2.16}$$

$$\sigma_{yy}^i = \left(1 + z_1 \tau_1 \frac{\partial}{\partial t}\right) \frac{\lambda^i}{\lambda + 2\mu} \frac{\partial u^i}{\partial x} - \left(1 + z_1 \tau_1 \frac{\partial}{\partial t}\right) \frac{\gamma^i}{\gamma} \theta^i \tag{4.2.17}$$

$$\left(1 + z_4 \tau_T \frac{\partial}{\partial t}\right) \frac{\kappa^i}{\kappa} \frac{\partial^2 \theta^i}{\partial x^2} = \left(1 + z_3 \tau_q \frac{\partial}{\partial t}\right) \left[\left(1 + z_2 \tau_0 \frac{\partial}{\partial t}\right) \left(\frac{\rho^i c^i}{\rho c} \frac{\partial \theta^i}{\partial t} + \frac{\gamma^i \gamma^2 T_0}{\gamma\,(\lambda + 2\mu)\,\rho c} \frac{\partial^2 u^i}{\partial t \partial x}\right) - \left(\frac{\rho_b c_b w_b}{\rho c c_0^2 \eta}\,(T_b - \theta^i)\right)\right] \tag{4.2.18}$$

$$\frac{\rho^i}{\rho} \frac{\partial^2 u^i}{\partial t^2} = \left(1 + z_1 \tau_1 \frac{\partial}{\partial t}\right) \frac{\lambda^i + 2\mu^i}{\lambda + 2\mu} \frac{\partial^2 u^i}{\partial x^2} - \left(1 + z_1 \tau_1 \frac{\partial}{\partial t}\right) \frac{\gamma^i}{\gamma} \frac{\partial \theta^i}{\partial x}. \tag{4.2.19}$$

Initial and boundary conditions can be expressed in the following dimensionless forms:

$$\theta^i\,(x, 0) = 0, \frac{\partial \theta^i}{\partial t}\,(x, 0) = 0, u^i\,(x, 0) = 0, \frac{\partial u^i}{\partial t}\,(x, 0) = 0 \tag{4.2.20}$$

$$\theta^I\,(0, t) = \theta_1 H\,(t)\,, \theta^{III}\,(L, t) = \theta_c, \sigma_{xx}^I\,(0, t) = \sigma_{xx}^{III}\,(L, t) = 0 \tag{4.2.21}$$

where $\theta_1 = \frac{(T_1 - T_0)}{T_0}, \theta_c = \frac{(T_c - T_0)}{T_0}$.

Above assumptions reduce the stress components and system of Eqs. (4.2.16-4.2.19) as

$$\sigma_{xx}^{i} = \mathcal{L}_{\lambda+2\mu}^{i}\left(1 + z_1\tau_1\frac{\partial}{\partial t}\right)\frac{\partial u^i}{\partial x} - \mathcal{L}_{\gamma}^{i}\left(1 + z_1\tau_1\frac{\partial}{\partial t}\right)\theta^i \tag{4.2.22}$$

$$\sigma_{yy}^{i} = \mathcal{L}_{\lambda}^{i}\left(1 + z_1\tau_1\frac{\partial}{\partial t}\right)\frac{\partial u^i}{\partial x} - \mathcal{L}_{\gamma}^{i}\left(1 + z_1\tau_1\frac{\partial}{\partial t}\right)\theta^i \tag{4.2.23}$$

$$\mathcal{L}_{k}^{i}\left(1 + z_4\tau_T\frac{\partial}{\partial t}\right)\frac{\partial^2\theta^i}{\partial x^2} = \left(1 + z_3\tau_q\frac{\partial}{\partial t}\right)\left[\left(1 + z_2\tau_0\frac{\partial}{\partial t}\right)\left(\mathcal{L}_{\rho}^{i}\mathcal{L}_{c}^{i}\frac{\partial\theta^i}{\partial t} + \mathcal{L}_{\gamma}^{i}\omega\frac{\partial^2 u^i}{\partial t\partial x}\right) - \left(\frac{\mathcal{L}_{\rho_B}\mathcal{L}_{c_B}w_b}{c_0^2\eta}\left(T_b - \theta^i\right)\right)\right] \tag{4.2.24}$$

$$\mathcal{L}_{\rho}^{i}\frac{\partial^2 u^i}{\partial t^2} = \left(1 + z_1\tau_1\frac{\partial}{\partial t}\right)\mathcal{L}_{\lambda+2\mu}^{i}\frac{\partial^2 u^i}{\partial x^2} - \left(1 + z_1\tau_1\frac{\partial}{\partial t}\right)\mathcal{L}_{\gamma}^{i}\frac{\partial\theta^i}{\partial x} \tag{4.2.25}$$

where

$$\mathcal{L}_{k}^{i} = \frac{k^i}{k}, \mathcal{L}_{\rho}^{i} = \frac{\rho^i}{\rho}, \mathcal{L}_{c}^{i} = \frac{c^i}{c}, \mathcal{L}_{\rho_B} = \frac{\rho_B}{\rho}, \mathcal{L}_{c_B} = \frac{c_B}{c},$$

$$\mathcal{L}_{\lambda+2\mu}^{i} = \frac{\lambda^i + 2\mu^i}{\lambda + 2\mu}, \mathcal{L}_{\lambda}^{i} = \frac{\lambda^i}{\lambda + 2\mu}, \mathcal{L}_{\gamma}^{i} = \frac{\gamma^i}{\gamma}, \omega = \frac{\gamma^2 T_0}{(\lambda + 2\mu)\,\rho c}.$$

Here, these linearized equations are solved by using the Laplace transform method. Using the homogeneous initial conditions prescribed by Eq. (4.2.22) in combination with the Laplace transform applied to both sides of Eqs. (4.2.22-4.2.25), we have

$$\overline{\sigma}_{xx}^{i} = (1 + z_1\tau_1 s)\left(\mathcal{L}_{\lambda+2\mu}^{i}\frac{\partial\overline{u}^i}{\partial x} - \mathcal{L}_{\gamma}^{i}\overline{\theta}^i\right) \tag{4.2.26}$$

$$\overline{\sigma}_{yy}^{i} = \left(1 + z_1\tau_1\frac{\partial}{\partial t}\right)\left(\mathcal{L}_{\lambda}^{i}\frac{\partial\overline{u}^i}{\partial x} - \mathcal{L}_{\gamma}^{i}\overline{\theta}^i\right) \tag{4.2.27}$$

$$(1+z_4\tau_T s)\,\mathcal{L}_k^i\frac{\partial^2\overline{\theta}^i}{\partial x^2}=(1+z_3\tau_q s)\left[\left(\mathcal{L}_\rho^i\mathcal{L}_c^i\,(1+z_2\tau_0 s)\,s+\mathcal{L}_{\rho_B}\mathcal{L}_{c_B}\frac{w_b}{c_0^2\eta}\right)\overline{\theta}^i\right.$$
$$\left.+\mathcal{L}_\gamma^i\omega\,(1+z_2\tau_0 s)\,s\frac{\partial\overline{u}^i}{\partial x}\right]-\frac{1}{s}\left(\mathcal{L}_{\rho_B}\mathcal{L}_{c_B}\frac{w_bT_b}{c_0^2\eta}\right) \tag{4.2.28}$$

$$\mathcal{L}_\rho^i s^2\overline{u}^i=(1+z_1\tau_1 s)\,\mathcal{L}_{\lambda+2\mu}^i\frac{\partial^2\overline{u}^i}{\partial x^2}-(1+z_1\tau_1 s)\,\mathcal{L}_\gamma^i\frac{\partial\overline{\theta}^i}{\partial x}. \tag{4.2.29}$$

Rewriting Eqs (4.2.28) and (4.2.29), we have

$$\frac{\partial^2\overline{\theta}^i}{\partial x^2}=\mathcal{L}_4\,(s)\left[\left(\mathcal{L}_1^i\right)\overline{\theta}^i+\mathcal{L}_2^i\frac{\partial\overline{u}^i}{\partial x}\right]-\mathcal{L}_3^i\,(s) \tag{4.2.30}$$

$$\frac{\partial^2\overline{u}^i}{\partial x^2}=\frac{\mathcal{L}_\rho^i s^2}{(1+z_1\tau_1 s)\,\mathcal{L}_{\lambda+2\mu}^i}\overline{u}^i+\frac{\mathcal{L}_\gamma^i}{\mathcal{L}_{\lambda+2\mu}^i}\frac{\partial\overline{\theta}^i}{\partial x} \tag{4.2.31}$$

where

$$\mathcal{L}_1^i\,(s)=\left(\frac{\mathcal{L}_\rho^i\mathcal{L}_c^i\,(1+z_2\tau_0 s)\,s+\mathcal{L}_{\rho_B}\mathcal{L}_{c_B}\frac{w_b}{c_0^2\eta}}{\mathcal{L}_k^i}\right),\mathcal{L}_2^i\,(s)=\frac{\mathcal{L}_\gamma^i\omega\,(1+z_2\tau_0 s)\,s}{\mathcal{L}_k^i};$$

$$\mathcal{L}_3^i\,(s)=\frac{1}{s\,(1+z_4\tau_T s)}\left(\frac{\mathcal{L}_{\rho_B}\mathcal{L}_{c_B}\frac{w_bT_b}{c_0^2\eta}}{\mathcal{L}_k^i}\right),\mathcal{L}_4\,(s)=\frac{(1+z_3\tau_q s)}{(1+z_4\tau_T s)}.$$

Eliminating terms $\overline{u^i}$ from Eqs. (4.2.30) and (4.2.31), we have

$$\frac{\partial^4\overline{\theta}^i}{\partial x^4}-\left[\mathcal{L}_4\,(s)\,\mathcal{L}_1^i\,(s)+\frac{\mathcal{L}_\rho^i s^2}{(1+z_1\tau_1 s)\,\mathcal{L}_{\lambda+2\mu}^i}+\mathcal{L}_4\,(s)\,\mathcal{L}_2^i\,(s)\,\frac{\mathcal{L}_\gamma^i}{\mathcal{L}_{\lambda+2\mu}^i}\right]\frac{\partial^2\overline{\theta}^i}{\partial x^2}+\left[\frac{\mathcal{L}_4\,(s)\,\mathcal{L}_1^i\,(s)\,\mathcal{L}_\rho^i s^2}{(1+z_1\tau_1 s)\,\mathcal{L}_{\lambda+2\mu}^i}\right]\overline{\theta}^i$$
$$=\frac{\mathcal{L}_3^i\,(s)\,\mathcal{L}_\rho^i s^2}{(1+z_1\tau_1 s)\,\mathcal{L}_{\lambda+2\mu}^i}$$

$$\left[\frac{\partial^4}{\partial x^4}-P_1^i\frac{\partial^2}{\partial x^2}+P_2^i\right]\overline{\theta}^i=\frac{\mathcal{L}_3^i\,(s)\,\mathcal{L}_\rho^i s^2}{(1+z_1\tau_1 s)\,\mathcal{L}_{\lambda+2\mu}^i} \tag{4.2.32}$$

where $P_1^i=\mathcal{L}_4\,(s)\,\mathcal{L}_1^i\,(s)+\frac{\mathcal{L}_\rho^i s^2}{(1+z_1\tau_1 s)\mathcal{L}_{\lambda+2\mu}^i}+\mathcal{L}_4\,(s)\,\mathcal{L}_2^i\,(s)\,\frac{\mathcal{L}_\gamma^i}{\mathcal{L}_{\lambda+2\mu}^i}$ and $P_2^i=\frac{\mathcal{L}_4(s)\mathcal{L}_1^i(s)\mathcal{L}_\rho^i s^2}{(1+z_1\tau_1 s)\mathcal{L}_{\lambda+2\mu}^i}$.

Here, we consider the $\pm R_j^i$ $(j = 1, 2$ ) as the roots of the given quadratic equation:

$$z^4 - P_1^i z^2 + P_2^i = 0.$$

Therefore, the complete solution of Eq. (4.2.32) can be written as

$$\overline{\theta}^i = A_1^i e^{R_1^i x} + A_2^i e^{-R_1^i x} + A_3^i e^{R_2^i x} + A_4^i e^{-R_2^i x} + K^i(s) \tag{4.2.33}$$

where $A_j^i\,(j = 1, 2, 3, 4)$ depends on parameter $s$ and $K^i(s) = \frac{\mathcal{L}_3^i(s)}{\mathcal{L}_4(s)\mathcal{L}_1^i(s)}$.
Similarly, we eliminate $\overline{\theta^i}$ from (4.2.30) and (4.2.31) to have

$$\frac{\partial^4 \overline{u}^i}{\partial x^4} - \left[\mathcal{L}_4(s)\,\mathcal{L}_1^i(s) + \frac{\mathcal{L}_\rho^i s^2}{(1 + z_1\tau_1 s)\,\mathcal{L}_{\lambda+2\mu}^i} + \mathcal{L}_4(s)\,\mathcal{L}_2^i(s)\,\frac{\mathcal{L}_\gamma^i}{\mathcal{L}_{\lambda+2\mu}^i}\right]\frac{\partial^2 \overline{u}^i}{\partial x^2} + \frac{\mathcal{L}_4(s)\,\mathcal{L}_1^i(s)\,\mathcal{L}_\rho^i s^2}{(1 + z_1\tau_1 s)\,\mathcal{L}_{\lambda+2\mu}^i}\overline{u}^i = 0. \tag{4.2.34}$$

Above equation can be written as

$$\left[\frac{\partial^4}{\partial x^4} - P_1^i\frac{\partial^2}{\partial x^2} + P_2^i\right]\overline{u}^i = 0. \tag{4.2.35}$$

Therefore, the general solution of eq. (4.2.35) can be represented as

$$\overline{u}^i = B_1^i e^{R_1^i x} + B_2^i e^{-R_1^i x} + B_3^i e^{R_2^i x} + B_4^i e^{-R_2^i x} \tag{4.2.36}$$

where $B_j^i\,(j = 1, 2, 3, 4)$ depends on parameter $s$.
With the help of Eqs. (4.2.33) and (4.2.36) in Eq. (4.2.31), we determine the relation between $A_j^i$ and $B_j^i$ as

$$B_1^i = \left[\frac{(1 + z_1\tau_1 s)\,\mathcal{L}_\gamma^i R_1^i}{(1 + z_1\tau_1 s)\,\mathcal{L}_{\lambda+2\mu}^i\left(R_1^i\right)^2 - \mathcal{L}_\rho^i s^2}\right]A_1^i,\; B_2^i = -\left[\frac{(1 + z_1\tau_1 s)\,\mathcal{L}_\gamma^i R_1^i}{(1 + z_1\tau_1 s)\,\mathcal{L}_{\lambda+2\mu}^i\left(R_1^i\right)^2 - \mathcal{L}_\rho^i s^2}\right]A_2^i,$$

$$B_3^i = \left[\frac{(1 + z_1\tau_1 s)\,\mathcal{L}_\gamma^i R_2^i}{(1 + z_1\tau_1 s)\,\mathcal{L}_{\lambda+2\mu}^i\left(R_2^i\right)^2 - \mathcal{L}_\rho^i s^2}\right]A_3^i,\; B_4^i = -\left[\frac{(1 + z_1\tau_1 s)\,\mathcal{L}_\gamma^i R_2^i}{(1 + z_1\tau_1 s)\,\mathcal{L}_{\lambda+2\mu}^i\left(R_2^i\right)^2 - \mathcal{L}_\rho^i s^2}\right]A_4^i. \tag{4.2.37}$$

Eq. (4.2.36) can be written as

$$\overline{u}^i = K_{11}^i e^{R_1^i x} A_1^i - K_{11}^i e^{-R_1^i x} A_2^i + K_{12}^i e^{R_2^i x} A_3^i - K_{12}^i e^{-R_2^i x} A_4^i \tag{4.2.38}$$

where

$$K_{11}^i = \left[ \frac{\left(1 + z_1 \tau_1 s\right) \mathcal{L}_\gamma^i R_1^i}{\left(1 + z_1 \tau_1 s\right) \mathcal{L}_{\lambda+2\mu}^i \left(R_1^i\right)^2 - \mathcal{L}_\rho^i s^2} \right], K_{12}^i = \left[ \frac{\left(1 + z_1 \tau_1 s\right) \mathcal{L}_\gamma^i R_2^i}{\left(1 + z_1 \tau_1 s\right) \mathcal{L}_{\lambda+2\mu}^i \left(R_2^i\right)^2 - \mathcal{L}_\rho^i s^2} \right].$$

Now we find out stress components with the help of Eqs. (4.2.26), (4.2.33) and (4.2.36) as

$$\overline{\sigma}_{xx}^i = K_{21}^i A_1^i e^{R_1^i x} - K_{21}^i A_2^i e^{-R_1^i x} + K_{22}^i A_3^i e^{R_2^i x} - K_{22}^i A_4^i e^{-R_2^i x} - \left(1 + z_1 \tau_1 s\right) \mathcal{L}_\gamma^i K^i \left(s\right) \tag{4.2.39}$$

where

$$K_{21}^i = \frac{\left(1 + z_1 \tau_1 s\right) \mathcal{L}_\gamma^i \mathcal{L}_\rho^i s^2}{\left(1 + z_1 \tau_1 s\right) \mathcal{L}_{\lambda+2\mu}^i \left(R_1^i\right)^2 - \mathcal{L}_\rho^i s^2}, K_{22}^i = \frac{\left(1 + z_1 \tau_1 s\right) \mathcal{L}_\gamma^i \mathcal{L}_\rho^i s^2}{\left(1 + z_1 \tau_1 s\right) \mathcal{L}_{\lambda+2\mu}^i \left(R_2^i\right)^2 - \mathcal{L}_\rho^i s^2}.$$

The boundary condition given by Eq. (4.2.21) can be expressed in Laplace transform domain as follows:

$$\overline{\theta}^I \left(0, s\right) = \frac{\theta_1}{s}, \overline{\theta}^{III} \left(L, s\right) = \frac{\theta_c}{s}, \overline{\sigma}_{xx}^I \left(0, s\right) = \overline{\sigma}_{xx}^{III} \left(L, s\right) = 0. \tag{4.2.40}$$

For simplicity, we consider the completely conductive and bounded skin tissue layers and therefore, we have

$$\overline{\theta}^i \left(L_i, s\right) = \overline{\theta}^{i+1} \left(L_i, s\right), \overline{q}^i \left(L_i, s\right) = \overline{q}^{i+1} \left(L_i, s\right),$$

$$\overline{\sigma}_{xx}^i \left(L_i, s\right) = \overline{\sigma}_{xx}^{i+1} \left(L_i, s\right), \overline{u}^i \left(L_i, s\right) = \overline{u}^{i+1} \left(L_i, s\right), \text{ for } i = 1, 2. \tag{4.2.41}$$

The coefficient $A_j^i$ $(j = 1, 2, 3, 4)$ are obtained with the help of boundary and interface conditions given by Eqs. (4.2.40) and (4.2.41). The Eqs. (4.2.33), (4.2.38)

and (4.2.39) represent the fundamental solution for the field variables in Laplace transform domain. These fundamental solutions are the combined solution for MGL and DPL generalized thermoelasticity theories and we can easily switch from one model to another by varying the values of parameters $z_1, z_2, z_3$ and $z_4$as mentioned above.

## 4.3 Numerical Results and Discussions

The displacement, temperature and stress components involve the complicated expressions of roots $R_j^i$ $(j = 1, 2)$ involving the Laplace transform parameter $s$. It seems practically formiddable task to obtain exact Laplace inversion solution for field variables. For this, the numerical inversion technique based on Stehfest algorithm is employed and this is implemented by using Matlab software. This section aims to discuss the transient thermal and mechanical responses of thermal load on skin tissue in the perspective of MGL generalized thermoelasticity theory. Results of present model are compared with the corresponding results in the context of DPL model. The following properties of a biological triple-layered skin tissue (Xu et al. (2008b)) are used in the numerical analysis as shown in table (4.1). The results are displayed graphically in various figures.

| ***Constants*** | ***Epidermis*** | ***Dermis*** | ***Subcutaneous fat*** | ***Blood*** |
|---|---|---|---|---|
| $\lambda\,(kg/ms^2)$ | $8.27 \times 10^8$ | $8.27 \times 10^7$ | $8.27 \times 10^4$ | |
| $\mu\,(kg/ms^2)$ | $3.446 \times 10^7$ | $3.446 \times 10^6$ | $3.446 \times 10^3$ | |
| $\rho\,(kg/m^3)$ | 1190 | 1116 | 971 | 1060 |
| $k\,(W/mK)$ | 0.235 | 0.445 | 0.185 | |
| $\alpha_t\,(C^{-1})$ | $10^{-4}$ | $10^{-4}$ | $10^{-4}$ | |
| $c\,(J/KgK)$ | 3600 | 3300 | 2700 | 3770 |

Table 4.1: The material parameters of triple layered skin tisue and blood (2008b)

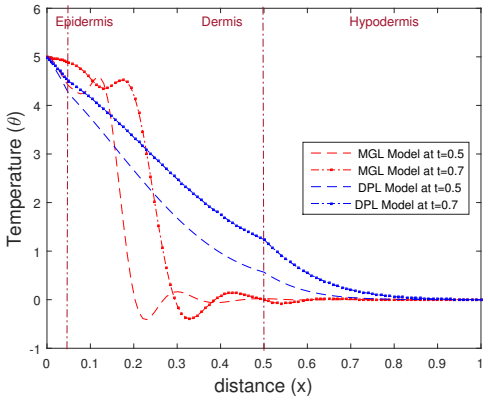


(a) Temperature variation

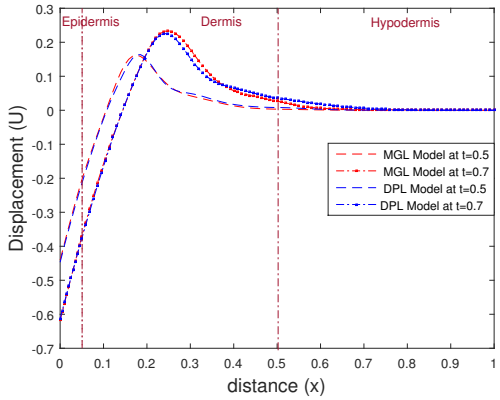


(b) Displacement variation

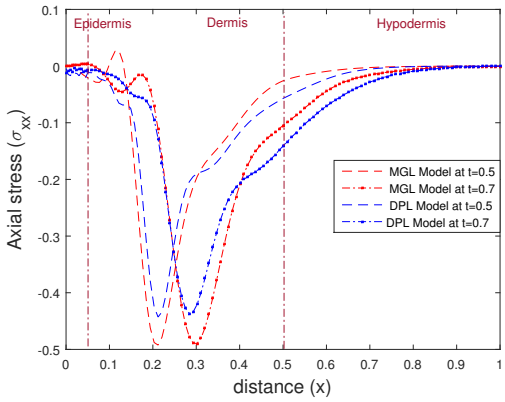


(c) Radial stress variation

Figure 4.3.1: Variation of field variables under DPL and MGL models at two different instant of time.

Figure (4.3.1) (a) depicts the dimensionless temperature response along the skin tissue depth under DPL and MGL model at different instants of time. Figures (4.3.2) provide a three-dimensional plot that illustrates how temperature varies with respects to skin tissue depth and time under the MGL and DPL models, respectively. The graphs clearly demonstrate that the temperature has the maximum value at the surface and satisfies the boundary condition. We notice for both the models that the amplitude of temperature have decreasing tendency with respect to tissue depth at specific instant of time. In MGL model, we observe temperature oscillation in dermis and hypodermis

layer but not in epidermis layer this is due to blood perfusion. This interpretation is consistent with the fact that blood perfusion is the primary physiological variable which enables tissue cooling.

This fact agrees with the experimental results reported by Mitra et al. (1995) and Roemer et al. (1985). Thus the temperature oscillations in graph must be the reflection of perfusion changes. It is noted that there is a significant difference in prediction of temperature by two the models. At any specific position of tissue, a predetermined period of time arrives when MGL model predicts sudden rise in temperature in the epidermis region, however this does not occur in DPL model. The effect of strain and temperature rates is therefore significant and MGL models predicts realistic results.

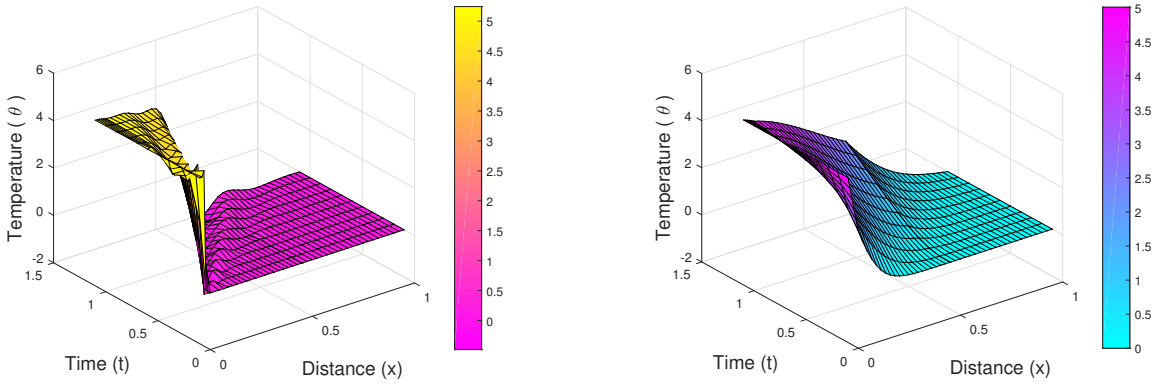


(a) MGL model

(b) DPL

Figure 4.3.2: Temperature variation with respect to time and position

Figure (4.3.1) (b) depicts the distribution of dimensionless displacement field along the skin tissue depth under DPL and MGL models at different instant of time. Figures (4.3.3) provide a three-dimensional plot that illustrates displacement field variation with respects to skin tissue depth and time using the MGL and DPL models, respectively. We note that, after a given distance from the skin's surface, the displacement field reaches its maximum value and as time goes on this peak value is attained at a greater distance with bigger amplitude. As it is clearly visible, displacement begins with negative value

and quickly rises to positive values. There is a prominent difference in prediction of displacement field too by two models, although the nature of variations is almost similar under both the models. Difference in prediction by two models increases with the increase in time. It is further noted that the maximum peak is attained near the epidermis region. The position of peak shifts towards dermis part of the skin as time passes.

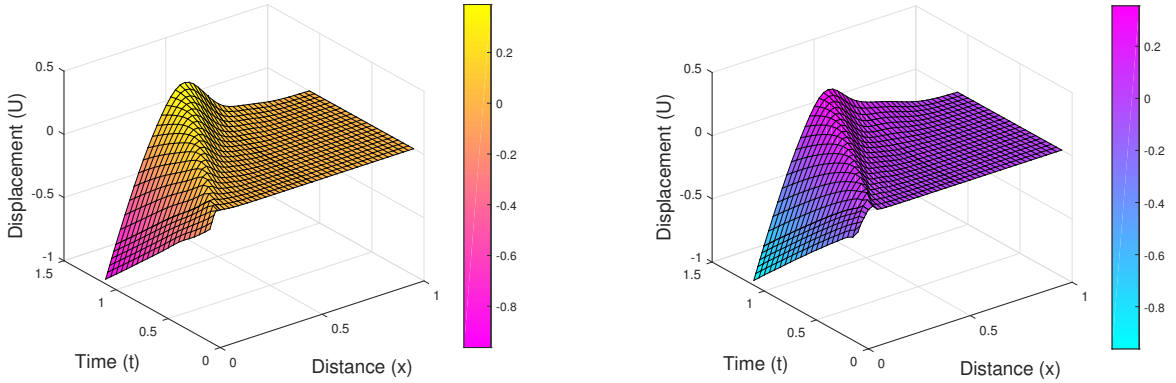


(a) MGL model (b) DPL

Figure 4.3.3: Displacement variation with respect to time and position

Figure (4.3.1) (c) depicts the distribution of dimensionless stress component $\sigma_{xx}$ along the skin tissue depth under DPL and MGL model at different instants of time. Figures (4.3.4) provide a three-dimensional plot that illustrates variation of stress component $\sigma_{xx}$ with respect to skin tissue depth and time using the MGL and DPL models, respectively. The boundary conditions are satisfied by the stress component. It is acknowledged that the stress components are compressive in character, and their absolute values progressively rise to achieve their peak values and then start decreasing to finally become zero. One can note that the peak value of absolute thermal stress shift towards the right (i.e., towards the dermis region) with time. One can further note that the skin tissue is more stressed under MGL model than it is in the DPL model. However,

oscillatory nature in stress component has been observed for small time under both the models.

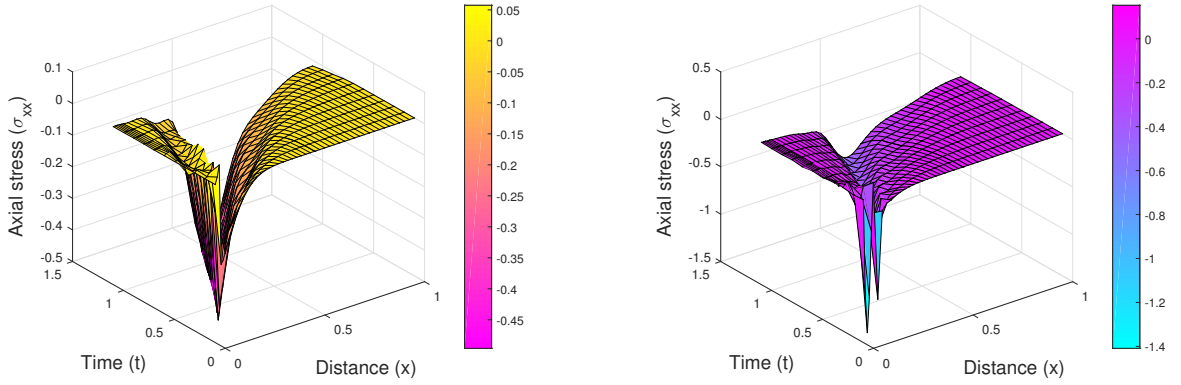


(a) MGL model (b) DPL model

Figure 4.3.4: Stress variation with respect to time and position

## 4.4 Conclusion

The aim of this chapter was to develop a mathematical model to investigate the thermo-mechanical phenomena occurring on triple-layered skin tissue by employing the Modified Green-Lindsay thermoelastic model (MGL) that takes into consideration of two thermal relaxation parameters in the constitutive relations. This thermoelastic model considers the effects of strain-rate and temperature-rate factors in thermoelastic behaviour and modifies the entropy relation and stress-strain temperature relation by keeping the Fourier law of heat conduction unchanged. The present investigation aims to study the effects of strain and temperature-rates in the thermoelastic behaviour of skin tissue by comparing the results with the results of the dual phase-lag thermoelastic model that also involves two phase-lag parameters in the modification of Fourier's heat conduction law. The present problem is therefore formulated in a unified way to derive the governing equations and constitutive relations under the present model and

also the DPL thermoelastic model. This work is believed to be beneficial for experts in bio-medical area to understand how one can choose most suitable and efficient generalized thermoelastic model as the solutions to cure the skin tissue disease through thermal loading which is highly reliant on the tissue-parameters. For heat transfer, the skin tissue consists of layered structure, each layer has distinct characteristic properties that are put together in a composite manner. A model is subsequently developed for computing the stresses and temperature that are induced layer-by-layer within the skin tissue during a thermal loading. The MGL model predicts significantly different temperature and thermal stress distribution in tissues in comparison to DPL heat conduction model. In biological skin tissues, the mechanism of temperature increment is analyzed during thermal therapy processing and MGL model predicts sharp increase in temperature at every position of tissue but after a certain interval of time. This model predicts larger compressive stress as compared to DPL model. This model, confirms the temperature oscillation at initial time stages which is practically reported by Mitra et al. (1995) and Liu et al. (1996; 1997) in their experiments, implying that MGL model may be more realistic than DPL model to study the thermoelastic behaviour of skin tissue. This further signifies that strain-rate and termperature terms can better model the present bio-thermomechanical problem.